Pergamon

Cement and Concrete Research 31 (2001) 389–395

CEMENT AND CONCRETE RESEARCH

Correlating laboratory and field tests of creep in high-performance concrete

Bertil Persson*

Division of Building Materials, Lund Institute of Technology, Box 118, 221 00 Lund, Sweden

Received 19 March 2000; accepted 20 December 2000

Abstract

This article outlines experimental laboratory and field studies on creep of young or mature high-performance concrete (HPC) carried out between 1991 and 1999. For this purpose, about 400 cylinders made out of eight mix compositions of HPC were studied in the laboratory. Half the number of HPC was sealed; half of the studies were carried out on air-cured HPC. Parallel tests on strength, internal relative humidity, RH and hydration were carried out on about 900 cubes that were made of HPC from the same batch as the cylinders were. Fragments from the strength tests were used to observe RH. Shrinkage was studied parallel to creep. The results and analyses of the laboratory studies show large influence of the maturity and of the mix composition of the HPC on the measured creep. The creep coefficient of HPC is smaller than in normal concrete. In contrast, shrinkage of HPC is somewhat larger than in normal concrete. The results obtained in the laboratory were correlated to field tests on 27 beams. The results in the field coincided well with the results in the laboratory studies. © 2001 Elsevier Science Ltd. All rights reserved.

Keywords: Cement; Concrete; Creep; High-performance concrete; Long-term performance; Shrinkage

1. Introduction and objectives

Shrinkage and creep of high-performance concrete (HPC) are two of the greater problems to be detected before HPC can be used in a large scale. A good review of the deformation properties of HPC is given by Jonasson and Persson [1]. Among other criteria, Jonasson and Persson [1] point out the difference in drying conditions of normal concrete and HPC. HPC mainly dries out in the surface while the internal part of a structure withholds the moisture for a very long time. The moisture conditions in HPC are dealt with in Refs. [2–6], particularly, that HPC dries out even when submerged for 7 years. The RILEM Data Bank (organized by Prof. Müller, Karlsruhe) contains few observations on HPC (the 28-day strength did not exceed 120 MPa). No correlation exists between real structures and laboratory tests in the Data Bank mentioned. An extensive study on more than 100 beams points out the great differences between laboratory tests and field results of creep and shrinkage [7]. The principal idea on how to design HPC as related to creep and shrinkage of normal concrete is summed up in Ref. [8]. However, until now, only one large test series exists correlating field data to laboratory tests of HPC with strength above 120 MPa [9–15].

The overall purpose of these experiments was to constitute values of the creep of HPC — quasi-instantaneous and short-term, including shrinkage, to be used in examination and discussion of the characteristic of HPC. The work was principally carried out according to Ref. [16]. It was also important to confirm the laboratory results by research in the field, which was done on beams.

2. Material and studied concretes

Appendix A shows the mix composition of the HPCs and the main property [9]. Using optimized mixes, an ideal grading curve and a correct mixing order, it was possible to carry out HPCs with good workability. Appendix B shows the characteristics of the aggregates used in the laboratory [17]. Appendix C shows the chemical composition of the cement [9]. The silica fume for the mix proportions with quartzite aggregate was granulated (fineness: 17.5 m^2/g, ignition losses: 2.3% by weight). For the

* Tel.: +46-46-222-4591; fax: +46-46-222-4427.

E-mail address: bertil.persson@byggtek.lth.se (B. Persson).

0008-8846/01/$ – see front matter © 2001 Elsevier Science Ltd. All rights reserved.
PII: S0008-8846(01)00455-0

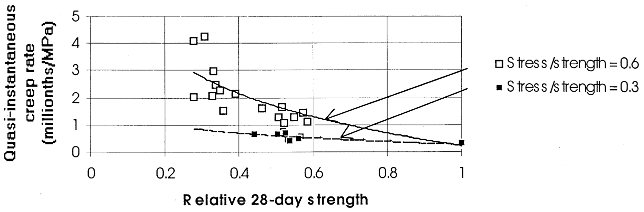

Fig. 1. Quasi-instantaneous creep rate of air-cured HPC.

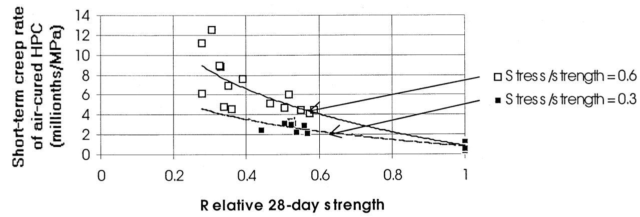

Fig. 3. Short-term creep rate of air-cured HPC.

remaining mix proportions and the field studies, a micro silica fume slurry was used (fineness: 22.5 m^2/g, ignition losses: 1.9% by weight).

3. Experimental

3.1. Creep

Quasi-instantaneous loading gave the possibility of estimating the initial strain (modulus of elasticity) and early creep. Shrinkage and creep were studied for cylinder 300 mm long with a diameter of 55 mm. Other properties of the HPC such as strength, hydration and RH were studied on cubes with a side of 100 mm and cylinders with a diameter of 55 mm and a length of 200 mm. The short-term creep was studied in an MTS machine for 66 h. The loading was adjusted within 0.015 s, i.e. quasi-instantaneously. The long-term creep was a study in common spring-loading devices by loading slowly at a rate of 1 MPa/s. The age of the HPC was 1, 2, 28 or 90 days at start of testing. (About 80 tests were started at 90 days of age [18].) At 1 and 2 days of age, the stress/strength ratio, σ/f_c, was 0.6; at 2, 28 and 90 days, it was 0.3. The rapid loading method also separated the elastic strain of the HPC from the viscous–elastic and the plastic part. After the quasi-instantaneous loading of the cylinders, the deformations were studied over a period of 66 h. The unloading of the cylinders was carried out within 1 s after a loading period of 66 h. The recovery was studied for 400 h. At this time, the recovery seemed to be finished except for the mature HPC. LVDT gauging and displacement transducers carried out the measurements. A mechanical device on specimens that were cast from the same batch as the specimen in use for the early creep study was used to measure the long-term creep. The loading of the long-term specimens was done parallel to the short-term tests. However, the long-term tests were continued after the short-term tests were finished, for at least 1 year and up to 5 years. After the loading period, the long-term recovery was measured. Parallel to all loading and unloading occasions, strength and RH was measured on cubes cast from the same batch as the creep specimens.

3.2. Shrinkage

Shrinkage was studied on cylinders made from the same batch as those used in the creep tests. Cast-in thermocouples measured the temperature development due to hydration (+4°C within 16 h of age) to compensate for the deformations due to temperature movements (the coefficient for thermal expansion was set at 1.1×10^{-5}). The specimens were weighed to control the moisture losses (or increase in case of carbonation). Self-desiccation of HPC caused a phenomenon called autogenous shrinkage, an unfavorable property of HPC. Autogenous shrinkage and consequently also self-desiccation occurs even under wet conditions due to the low permeability of HPC [5]. The RH at self-desiccation was measured parallel to the shrinkage. RH at drying of the HPC was measured in order to ensure that the internal part of the cylinders obtained ambient RH = 60%, thus, that shrinkage came to an end.

4. Results

Fig. 1 shows the quasi-instantaneous creep rate of air-cured HPC [9]. Fig. 2 shows the quasi-instantaneous creep rate of sealed HPC until 2 s of loading. The early creep rate seems to be constant at a certain age (maturity) of the HPC. It was then fairly independent of the water–cement ratio. However, the initial strain (elastic strain) at rapid load was dependent on the water–cement ratio, w/c. Figs. 3 and 4 show the continued short-term creep rate from 2 s until 66 h of loading. Finally, Figs. 5 and 6 show the long-term creep

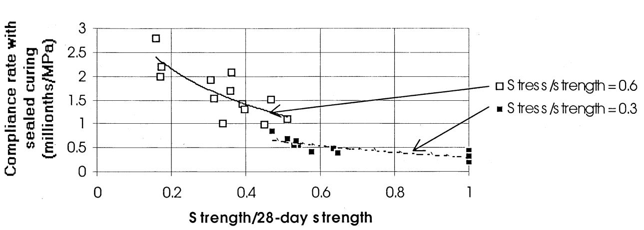

Fig. 2. Quasi-instantaneous creep rate of sealed HPC.

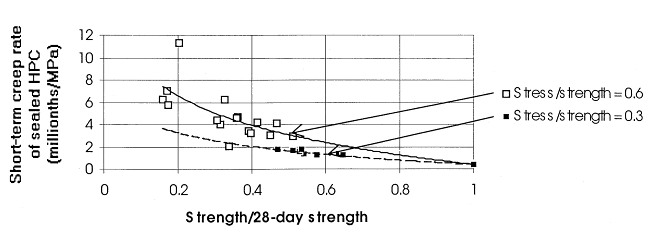

Fig. 4. Short-term creep rate of sealed HPC.

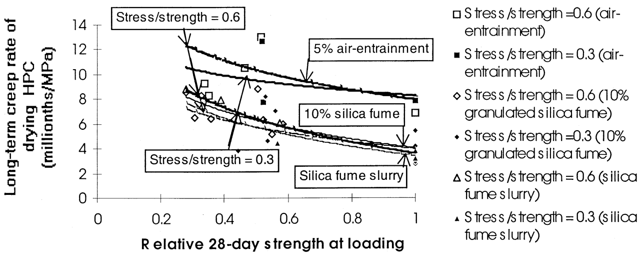

Fig. 5. Long-term creep rate of air-cured HPC.

rate from 1 day until 1000 days of age. The long-term creep rate was more affected by w/c than the short-term creep. The strength at loading had a dominating effect on both the quasi-instantaneous and the short-term creep rate [9]. Before the calculation of creep, the shrinkage was continuously withdrawn. Fig. 7 shows the long-term shrinkage after 3–4 years measured on cylinders made from the same batch of concrete [9,10].

5. Analysis

5.1. Shrinkage

Parallel studies of RH and shrinkage showed that the shrinkage had come to an end after about 1 year. Eq. (1) gives the autogenous shrinkage related to RH ($0.7 < \mathrm{RH} < 0.9$) [10]:

$$\varepsilon_{\mathrm{B}} = k_{\mathrm{sRH}} 1.75(1 - 1.13\mathrm{RH}) \quad R^2 = .72 \tag{1}$$

$k_{\mathrm{sRH}} = 1.3$ for silica fume slurry; $k_{\mathrm{sRH}} = 1$ for granulated silica fume; R^2 denotes a correlation coefficient ($R^2 > .50$); and ε_{B} denotes autogenous shrinkage (mm/m).

The different kinds of shrinkage (after 3–4 years) were related to w/c [10]:

$$\varepsilon = 34k((\mathrm{w/c})^2 - 0.68(\mathrm{w/c}) + 0.13) \quad R^2 = .80 \tag{2}$$

$$\varepsilon_{\mathrm{B}} = 1.5k_B(0.43 - (\mathrm{w/c})) \quad R^2 = .75 \tag{3}$$

$$\varepsilon_{\mathrm{C}} = 0.85((\mathrm{w/c}) - 0.25) \quad R^2 = .50 \tag{4}$$

$$\varepsilon_{\mathrm{D}} = 33((\mathrm{w/c})^2 - 0.654(\mathrm{w/c}) + 0.115) \quad R^2 = .52 \tag{5}$$

$k = 1.1$ for HPC with 10% silica fume slurry; $k = 1$ for HPC with 10% granulated silica fume or 5% silica fume slurry;

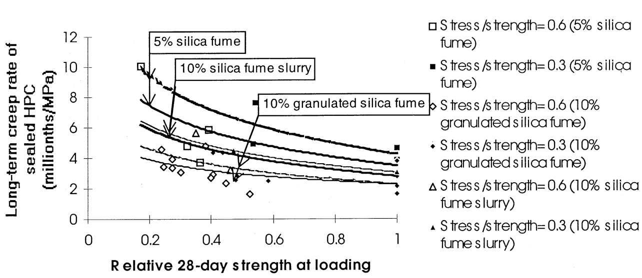

Fig. 6. Long-term creep rate of sealed HPC.

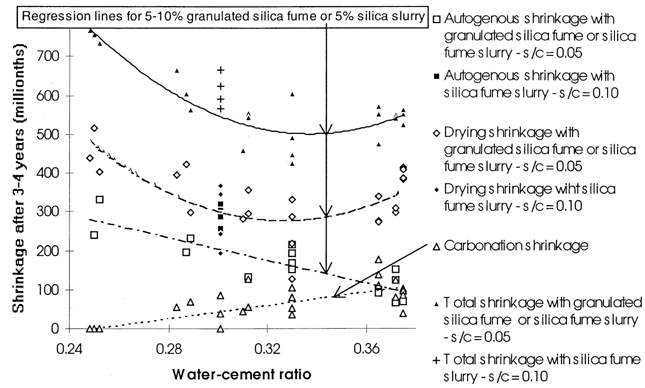

Fig. 7. Long-term shrinkage of HPC.

$k_{\mathrm{B}} = 1.5$ (10% silica fume slurry); $k_{\mathrm{B}} = 1$ (10% granulated silica fume or 5% slurry); ε, ε_{B}, ε_{C}, ε_{D} denote total, autogenous, carbonation or drying shrinkage, respectively (mm/m).

The driving force for the shrinkage was the internal force caused by desiccation [11]. The time dependence of shrinkage was expressed by Eq. (6) [18]:

$$\varepsilon_t = [0.2k\ln(t) + 1]\varepsilon_{\mathrm{l}} \quad R^2 = .72 \tag{6}$$

$k_t = 1.3$ for sealed HPC, $k = 1.0$, otherwise; $\ln(t)$ natural logarithm of time (years); ε_t shrinkage vs. time (mm/m); and ε_{l} long-term shrinkage according to Eqs. (2)–(5).

5.2. Elastic modulus

The elastic modulus was estimated from experiments with quasi-instantaneous loading [19]:

$$E_{\mathrm{B}} = \{6.06 - 3.02(\sigma/f_{\mathrm{c}}) - (0.44 - 0.51(\sigma/f_{\mathrm{c}}))\ln(t - t')\} \times (f_{\mathrm{c}})^{0.42+0.061(\sigma/f_{\mathrm{c}})-0.039(\sigma/f_{\mathrm{c}}-0.5)\ln(t-t')} \quad R^2 = .66 \tag{7}$$

$$E_{\mathrm{D}} = \{10.7 - 12.8(\sigma/f_{\mathrm{c}}) - (0.15 + 0.29(\sigma/f_{\mathrm{c}}))\ln(t - t')\} \times (f_{\mathrm{c}})^{0.18+0.61(\sigma/f_{\mathrm{c}})0.022(\sigma/f_{\mathrm{c}}-0.1)\ln(t-t')} \quad R^2 = .73 \tag{8}$$

f_{c} denotes the 100-mm cube strength at loading (MPa) $\{20 < f_{\mathrm{c}} < 120\ \mathrm{MPa}\}$; $\ln(t - t')$ denotes the natural logarithm of the time elapsed from loading (s); E_{B} denotes the elastic modulus of HPC with sealed curing (GPa); E_{D} denotes the elastic modulus of HPC with air curing (GPa); and σ/f_{c} denotes the stress to cube strength ratio at loading $\{0.3 < \sigma/f_{\mathrm{c}} < 0.6\}$.

5.3. Creep compliance

The estimation of creep compliance included the following parts obtained by addition:

1. The elastic part according to Eqs. (7) and (8);
2. Quasi-instantaneous creep compliance from loading until 2 s of loading;

3. Short-term creep compliance from 0.0005 until 66 h of loading; and
4. Long-term creep compliance from 2.7 days until the end of loading.

Initially, the quasi-instantaneous creep rate was estimated according to Figs. 1 and 2:

$$a_B = (0.18 + 0.42(\sigma/f_c))s_5 + (0.12 - 2(\sigma/f_c))\ln(f_c/f_{c28}) \quad R^2 = .68 \tag{9}$$

$$a_D = (0.37 - 0.23(\sigma/f_c))s_{a5} + (1.2 - 5.5(\sigma/f_c))\ln(f_c/f_{c28}) \quad R^2 = .78 \tag{10}$$

a_B denotes the quasi-instantaneous creep rate with sealed curing (millionths/MPa); a_D denotes the quasi-instantaneous creep rate with air curing (millionths/MPa); f_c/f_{c28} relative strength level $\{\sigma/f_c=0.3$: $0.4<f_c/f_{c28}<1$; $\sigma/f_c=0.6$: $0.15<f_c/f_{c28}<0.5\}$; $\ln(f_c/f_{c28})$ denotes the natural logarithm of the relative 28-day cube strength; $s_{a5}=1.1$ for HPC with 5% silica fume or/and air entrainment; $s_{a5}=1$ for HPC with 10% silica fume and no air entrainment; $s_5=1.5$ for HPC with 5% silica fume; $s_5=1$ for 10% silica fume; and σ/f_c denotes the stress/cube strength ratio at loading $\{0.3<\sigma/f_c<0.6\}$.

Then, the short-term creep rate was estimated according to Figs. 3 and 4 [9]:

$$a_B = 0.14((w/c) + 2.5)s_5 + (0.29 - 6.9(\sigma/f_c))\ln(f_c/f_{c28}) \quad R^2 = .83 \tag{11}$$

$$a_D = 3.4((w/c) - 0.13)s_{a5} + (0.3 - 11(\sigma/f_c))\ln(f_c/f_{c28}) \quad 0.25 < w/c < 0.40; \; R^2 = .73 \tag{12}$$

a_B denotes the creep rate of sealed HPC (millionths/MPa); a_D denotes the rate short-term creep of drying HPC (millionths/MPa); f_c/f_{c28} denotes the relative 28-day strength at loading $\{0.3<f_c/f_{c28}<1\}$; $\ln(f_c/f_{c28})$ denotes the natural logarithm of the relative strength when loading $\{0.4<f_c/f_{c28}<1$ for $\sigma/f_c=0.3$ and $0.15<f_c/f_{c28}<0.5$ for $\sigma/f_c=0.6\}$; $s_{a5}=1.5$ for 5% silica fume and/or air entrainment; $s_{a5}=1$ for 10% silica fume; $s_5=1.25$ for HPCs with 5% silica fume or/and air entrainment (10% silica fume); $s_{a5}=1$ for HPC with 10% silica fume; and σ/f_c denotes the stress/strength (100-mm cube) ratio at loading $\{0.3<\sigma/f_c<0.6\}$.

Finally, the long-term creep rate was estimated according to Figs. 5 and 6 [9]:

$$a_B = 231k_{s5}((w/c)^2 - 0.594(w/c) + 0.0952) - k_{s5}(2.83 - 3(\sigma/f_c))\ln(f_c/f_{c28}) \quad R^2 = .67 \tag{13}$$

$$a_D = 513k_{ai}((w/c)^2 - 0.6(w/c) + 0.0959) - k_{as}(1.83 + 2.37(\sigma/f_c))\ln(f_c/f_{c28}) \quad R^2 = .71 \tag{14}$$

a_B denotes long-term creep rate with sealed curing (millionths/MPa); a_D denotes long-term creep rate with air curing (millionths/MPa); f_c denotes cube strength at loading (MPa); f_{c28} denotes 28-day cube strength (MPa); $k_{ai}=1.5$ for HPC with 5% air entrainment, $k_{ai}=1$, otherwise; $k_{as}=0.8$ with 5% air entrainment, $k_{as}=1.3$ with silica fume slurry, $k_{as}=1$, otherwise; and $k_{s5}=1.5$ with 5% silica fume or 10% silica fume slurry, $k_{s5}=1$, otherwise.

5.4. Dimensional effect

The effect on creep and shrinkage of the size of the specimen was investigated by parallel studies on cylinders, 55 and 100 mm in diameter [9]. One hundred 100-mm cylinders and more than three hundred 55-mm cylinders gave the following dimensional effect on HPC [9]:

$$J_{tot} = J_B \pm ((V/A)_{cyl}/(V/A)_{beam})(J_D - J_B) \tag{15}$$

A denotes the cross-sectional area of the specimen; J_{tot} denotes the total compliance taking in account the size effect; J_B denotes compliance of the sealed cylinder 55 mm in diameter; J_D denotes compliance at drying of the cylinder 55 mm in diameter; V denotes the area of the specimen; and V/A half the hydraulic radius to be calculated ($V/A=0.014$ m for 55-mm cylinders).

5.5. Creep coefficient

For HPC that was mature when it was loaded, the creep coefficient after 4 years varied between 1.1 (sealed curing) and 1.3 (air curing), i.e. smaller than for normal concrete. The viscous–elastic part of the creep coefficient was hardly detectable at w/c < 0.35. The total creep compliance, J_{tot}, may be estimated by addition of the different parts, Eqs. (7)–(14). For HPC that was young when loading, the creep coefficient was estimated according to (Eqs. (16)–(18)) [9]:

$$(J_{pl}/J_{el})_D = 50k_{mai}k_{m5}((w/c)^2 - 0.68(w/c) + 0.1372) - 7.8k_{yai}k_{ysl}(\sigma/f_c)\ln(f_c/f_{c28}) \quad R^2 = .72 \tag{16}$$

$$(J_{pl}/J_{el})_B = 82k_{msl}((w/c)^2 - 0.544(w/c) + 0.0824) + 49(\sigma/f_c)k_{ys1}e^{-6.77k((\sigma/f_c)+0.451)(f_c/f_{c28})} \quad R^2 = .8 \tag{17}$$

$$J_{vi}/J_{el} = 0.75k_{mD}((w/c) - 0.25) - k_{yD}\ln(f_c/f_{c28}) \quad R^2 = .85 \tag{18}$$

ai denotes 5% air entrainment; m denotes mature HPC; k, k_{mai}, k_{msl}, k_{mD}, k_{m5}, k_{yai}, k_{ysl} and k_{yD} denote constants in Table 1 ($k=1$, otherwise); sl denotes silica fume slurry; y

Table 1
Constants in Eqs. (16)–(18) ($k=1$, otherwise)

Constant	k (slurry)	k_{mai}	k_{msl}	k_{mD}	k_{m5}	k_{yai}	k_{ysl}	k_{yD}
Air curing	–	1.38	–	1.66	1.33	0.52	1.48	0
Sealed curing	1.1	–	1.56	1	–	–	2	− 0.06

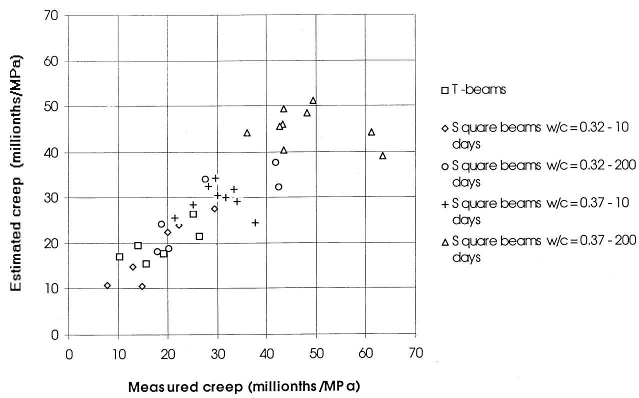

Fig. 8. Creep estimated according to Eqs. (9)–(15) vs. the creep measured in the field.

denotes HPC young when loading; B denotes sealed curing; D denotes air curing; J_{pl}/J_{el} denotes ratio of viscous–plastic compliance to the elastic compliance; J_{vi}/J_{el} denotes ratio of viscous–elastic compliance to the elastic compliance; σ denotes stress (MPa); and 5 denotes HPC with 5% silica fume.

6. Field tests

After the laboratory studies were finished, 20 square beams (200 × 200 mm) and seven T-beams (350 mm wide and 300 mm high) were cast. The concrete of the beams in the field tests had w/c varying between 0.27 and 0.37 (corresponding strength: 120 and 80 MPa). Parallel studies on shrinkage were carried out on cylinders, both sealed and air-cured [9]. The measured shrinkage was about 25% larger than the shrinkage estimated according to Eqs. (2)–(5), which may be due to the finer type of cement in use. However, the effect of the aggregate content was small since it was held at about 0.72, both in the laboratory and in the field tests [20]. The creep studies on the beams were carried out for 200 days. Fig. 8 shows the creep estimated according to Eqs. (9)–(15) vs. the creep measured in the field. The measured creep was on average 90% of the estimated creep, which is reasonably good [9].

7. Summary and conclusions

About 400 cylinders and 900 cubes made out of eight mix compositions of HPC were studied for 5 years. The cylinders were loaded at 1, 2, 28 or 90 days of age. Studies were carried out on quasi-instantaneous creep, short-term creep and long-term creep. The stress/cube strength ratio at loading was 0.3 or 0.6. Strength tests were carried out on the cubes. Fragments from the strength tests were used to observe the internal relative humidity. Shrinkage was studied parallel to the creep studies. Half the number of HPC was sealed. As reference, studies were also carried out on air-cured HPC. The results and analyses show the following results:

- Early deformations were analyzed by quasi-instantaneous loading in the laboratory (2 s).
- The short compliance was correlated to studies over 2 days.
- Long-term creep was analyzed after 4 years of creep and shrinkage studies.
- The laboratory tests were well correlated to field tests on 27 beams.

Acknowledgments

Financial support by the Swedish–Norwegian Consortium for Research on HPC is gratefully acknowledged. I am also grateful to Professor Göran Fagerlund for his supervision.

Appendix A. Mix composition of the fresh HPC and strength at various ages

Material/mix number	1	1 (3)	2	3	4	5	6	7	8
Quartzite, 8–11 mm	460	440							
Quartzite, 11–16 mm	460	440	965	910		1010	985		1065
Sand, Åstorp 0–8 mm	800	780	820	790		750	755		690
Granite, Norrköping 11–16								1030	
Gravel, Toresta 8–16 mm					1095				
Natural sand, Bålsta 0–8					780			780	
Cement, Degerhamn Std	430	410	440	445	455	495	530	490	545
Granulated silica fume	21	21	44	45		50	51		55
Silica fume slurry					23			49	
Air-entraining agent	0.02	0.04		0.02					
Superplasticizer, melamine	2.6	2.8	4.5	3.8	5.1	4.6	7.6	8.6	10.8
Water–cement ratio	0.38	0.38	0.37	0.37	0.33	0.31	0.30	0.30	0.25
Air content (vol.%)	4.8	7.0	1.1	4.0	0.9	1.1	1.2	1.0	1.3

Aggregate content (vol.%)	0.74	0.74	0.73	0.72	0.75	0.71	0.70	0.72	0.70
Aggregate/cement ratio	4	4	4.1	3.8	4.1	3.6	3.3	3.7	3.2
Density (kg/m^3)	2335	2245	2440	2360	2510	2465	2480	2500	2490
Slump (mm)	140	140	160	170	45	200	130	45	45
28-day drying strength (MPa)	69	50	85	69	89	99	106	112	114
1-year drying strength (MPa)	70	54	89	76	97	109	112	121	125
3-year drying strength (MPa)	69		91		97		115	121	127
28-day sealed strength (MPa)	89	62	105	95	101	121	126	122	129
1-year sealed strength (MPa)	101	65	117	98	115	129	145	131	154
2-year sealed strength (MPa)	112				115			131	
3-year sealed strength (MPa)			123	102			141		145
4-year sealed strength (MPa)	102				113			129	

Appendix B. Characteristics of the aggregates [17]

Material/ characteristics	Modulus of elasticity (GPa)	Compressive strength (MPa)	Split tensile strength (MPa)	Ignition losses (%)
Quartzite sandstone	60	330	15	0.3
Natural sand				0.8
Granite	61	150	10	1.7
Pea gravel				1.6
Crushed sand	59	230	14	2

Appendix C. Chemical composition and the main characteristics of the cement [9]

Low-alkali cement type Degerhamn	Standard	P 400
X-ray fluorescence analysis (%)		
CaO	64.9	64.0
SiO_2	22.2	22.0
Al_2O_3	3.36	3.71
Fe_2O_3	4.78	4.80
MgO	0.91	0.91
ICP analysis (%)		
K_2O	0.56	0.55
Na_2O	0.04	0.04
LECO apparatus (%)		
Ignition losses at 950°C	0.63	0.63
SO_3	2.00	2.22
Physical properties		
Specific surface according to Blaine (m^2/kg)	302	404
Density (kg/m^3)	3220	3210
Setting time		
Vicat (min)	135	95
Water (%)	26.0	26.8
Standard test (prisms 40 × 40 × 160 mm, MPa)		
1 day	11.0	16.2
2 days	20.2	25.4
7 days	35.8	41.3
28 days	52.6	59.5

References

[1] J.-E. Jonasson, B. Persson, Creep, Design Handbook. The Consortium for Research of HPC Structures, Technical University of Luleå, Luleå, 1998, pp. 2.7–2.17.

[2] B. Persson, Hydration and strength of HPC, ACBM 3 (1996) 107–123.

[3] B. Persson, Self-desiccation and its importance in concrete technology, Mater. Struct. 30 (1997) 293–305.

[4] B. Persson, Moisture in concrete subjected to different kinds of curing, Mater. Struct. 30 (1997) 533–544.

[5] B. Persson, Self-desiccation and its importance in concrete technology, Nord. Concr. Res. 20 (1998) 120–129.

[6] B. Persson, Seven-year study of the effect of silica fume in concrete, ACBM 7 (1998) 139–155.

[7] K. Sakata, Prediction of concrete creep and shrinkage, in: Z. Baźant, I. Carol (Eds.), Proceedings of the Fifth International RILEM Symposium on Creep and Shrinkage in Barcelona, E & FN Spon, London, 1993, pp. 649–654.

[8] H.S. Müller, K. Küttner, Characteristics and prediction of creep of HPC, in: F.H. Wittmann, P. Schwesinger (Eds.), Proceedings of the Fourth Weimar Workshop held at HAB, Weimar, Freiburg and Unterengstringen, Germany and Switzerland, 1995, pp. 145–162.

[9] B. Persson, Quasi-instantaneous and Long-term Deformations of HPC with Some Related Properties, Doctoral Thesis, Report TVBM-1016, Lund Institute of Technology, Lund, 1998, 500 pp.

[10] B. Persson, Shrinkage of HPC, in: E. Tazawa (Ed.), Proceedings of the International Workshop on Autogenous Shrinkage of Concrete, Hiroshima, E & FN Spon, London and New York, 1998, pp. 101–118.

[11] B. Persson, Chemical shrinkage and self-desiccation in portland cement based mortars, Concr. Sci. Eng. 1 (1999) 228–237.

[12] B. Persson, Long-term shrinkage of HPC, in: H. Justnes (Ed.), Proceedings of the 10th International Congress on the Chemistry of Cement, Amarkai Ltd. and Congree Gothenburg Ltd., Gothenburg, 1997, (Contribution 2ii073, Gothenburg, 9 pp.).

[13] B. Persson, Basic deformations of high-performance concrete at early ages, Nord. Concr. Res. 20 (1997) 59–74.

[14] B. Persson, Experimental studies on shrinkage in HPC, Cem. Concr. Res. 28 (1998) 1023–1036.

[15] B. Persson, Quasi-instantaneous and long-term deformations of HPC with sealed curing, ACBM 8 (1998) 1–16.

[16] P. Acker, Creep and shrinkage of concrete, in: Z. Baźant, I. Carol (Eds.), Proceedings of the Fifth International RILEM Symposium on Creep and Shrinkage in Barcelona, E & FN Spon, London, 1993, pp. 3–14.

[17] M. Hassanzadeh, Fracture Mechanical Properties of HPC. Report M4:05. Lund Institute of Technology, Lund, 1994, pp. 9–15.

[18] B. Persson, Deformations of House Construction Concrete — Effect of Production Methods on Elastic Modulus, Creep and Shrinkage, Report TVBM-3088, Lund Institute of Technology, Lund, 1999, 71 pp.

[19] B. Persson, Creep recovery and elastic modulus of high performance concrete, Concr. Sci. Eng. 2 (2000) 78–87.

[20] E. Tazawa, S. Miyazawa, Effect of constituents and curing conditions on autogenous shrinkage of concrete, in: E. Tazawa (Ed.), Proceedings of the International Workshop on Autogenous Shrinkage of Concrete, Hiroshima, E & FN Spon, London and New York, 1998, 269–280.